ANALYSIS OF COMPOSITES WITH RIGID REINFORCEMENTS BY THE BOUNDARY ELEMENT METHOD

R. Górski[1*], P. Fedeliński[1]

[1]*Department of Strength of Materials and Computational Mechanics, Silesian University of Technology, Konarskiego 18A, 44-100 Gliwice*
**e-mail: Radoslaw.Gorski@polsl.pl*

Keywords: boundary element method, rigid inclusions, rigid-line, rigid-surface.

Abstract
In the paper two-dimensional (2D) and three-dimensional (3D) elastic bodies reinforced by rigid-line or rigid-surface inclusions are analyzed by the boundary element method (BEM). Displacements and tractions are compared for 2D and 3D models and also with solutions obtained by the finite element method (FEM) and good agreement of the results is obtained. The formulation is very attractive and efficient in terms of an input data and the number of degrees of freedom reduction. The method can be used in modeling of composites with very stiff reinforcement in comparison with a matrix which are in the form of fiber-like or flake-like particles. Nanocomposites reinforced by carbon nanotubes, graphene layers or other stiff particles are such the exemplary materials.

1 Introduction

Composite materials are strengthened by different kinds of reinforcements in order to improve their overall properties. Very often the reinforcement has a form of spherical particles, fiber-like or flake-like shapes. If the stiffness of the reinforcement is much larger than the stiffness of a matrix, the former can be modeled as rigid and the latter as deformable. Nanocomposites are the representative materials where such a big difference of the mechanical properties is present. In these materials, a soft matrix is usually reinforced by very stiff particles (e.g. spherical fullerens, carbon nanotubes, graphene layers, nanoclays, etc.).

Problems dealing with a single or multiple rigid inhomogeneities have been studied by many authors. Displacement, traction and stress fields, interfacial stresses and fractures, load transfer mechanisms, the overall mechanical properties and other problems in composites with rigid particles have been investigated both analytically and numerically. Ballarini [1] for instance has presented the solution to the problem of a rigid-line inhomogeneity by an integral equation approach. He concluded that the stresses at the tips of the inhomogeneity are singular, similar as in a crack problem. Pingle et al. [2] have derived the rigid-line inclusion solutions from the crack solutions and analyzed stress fields and the load transfer mechanisms for a single and multiple inclusions. Gorbatikh et al. [3] have shown a relation between elastic properties and stress intensity factors for composites with rigid-line inclusions.

High gradients of stresses present at the tips of rigid inhomogeneities should be accurately determined. Apart from the analytical investigations, which are applicable usually for simple geometries and boundary conditions, numerical methods can be used. The boundary element method (BEM) allows accurately analyzing the problems with high concentrations of stresses

[4]. It is also very efficient and relatively easy to use in analysis of composites with many reinforcements of arbitrary shapes, which can be rigid or deformable.
The analysis of elastic properties of composites with deformable carbon nanotubes of arbitrary shapes by the coupled BEM/FEM is shown for instance by Górski [5]. Two-dimensional representative volume elements of the material have been considered in order to analyze the properties. Fedeliński [6, 7] has shown the analysis of two-dimensional elastic bodies with a single or multiple rigid-line inclusions by the BEM. He considered an interaction between a rigid inclusion and a crack, stress fields near the inclusions and also determined the effective properties of composites with multiple fibers. Liu et al. [8, 9] have also analyzed composites numerically using a 3D rigid-inclusion model and the fast multipole BEM. They have studied a single rigid sphere or multiple rigid fibers in a matrix. The results have been compared with an analytical solution for a rigid sphere and an excellent agreement has been obtained for displacements and stresses. Most of the presented models of composites based on the rigid-inclusion assumption and the BEM are two-dimensional.
In the present paper the composites containing rigid particles are analyzed by the BEM. The fiber-like or platelet-like shapes are considered using a 2D rigid-line or a 3D rigid-surface models, respectively. Both models can be used in analysis of composites containing the platelet-like reinforcements with high length to thickness ratio and fiber to matrix stiffness ratio. Such composites (for instance naturally occurring composites [2]) have been usually analyzed by the BEM using 2D rigid-line models. The aim of the paper is to extend and verify the formulation for 3D bodies containing planar rigid-surface inclusions.

2 Formulation

A 3D homogeneous, isotropic and linear-elastic body loaded by boundary tractions **t** applied on its outer surface and by body forces **b** is considered. The outer boundary of the body is denoted by Γ and its domain by Ω. The relation between displacements and loading can be expressed in the following form [4]:

$$\mathbf{c}(\mathbf{x})\mathbf{u}(\mathbf{x})+\int_{\Gamma}\mathbf{T}(\mathbf{x},\mathbf{y})\,\mathbf{u}(\mathbf{y})\;\mathrm{d}\Gamma(\mathbf{y})=\int_{\Gamma}\mathbf{U}(\mathbf{x},\mathbf{y})\,\mathbf{t}(\mathbf{y})\;\mathrm{d}\Gamma(\mathbf{y})+\int_{\Omega}\mathbf{U}(\mathbf{x},\mathbf{y})\,\mathbf{b}(\mathbf{y})\;\mathrm{d}\Omega(\mathbf{y}) \qquad (1)$$

where **u** and **t** are the displacement and traction vectors, respectively, **U**(**x**,**y**) and **T**(**x**,**y**) are respectively the displacement and traction fundamental solutions of elastostatics, **x** is a source (collocation) point and **y** is any point on the external boundary of the body or in its domain. The matrix **c**(**x**) depends on a position of the collocation point **x**.
Assume that the body is reinforced by a planar zero-thickness inclusion perfectly bonded to it. In the present formulation, the inclusion can have an arbitrary shape and thus the generic name – the rigid-surface inclusion – will be interchangeably used together with a flat inclusion or a planar inclusion in the subsequent part of the paper. When the body is loaded interaction forces between the body and inclusion occur. They are treated as particular body forces acting along the surface of the inclusion. The relation (1) can be now written in the following form:

$$\mathbf{c}(\mathbf{x})\mathbf{u}(\mathbf{x})+\int_{\Gamma}\mathbf{T}(\mathbf{x},\mathbf{y})\,\mathbf{u}(\mathbf{y})\;\mathrm{d}\Gamma(\mathbf{y})=\int_{\Gamma}\mathbf{U}(\mathbf{x},\mathbf{y})\,\mathbf{t}(\mathbf{y})\;\mathrm{d}\Gamma(\mathbf{y})+\int_{\Gamma_i}\mathbf{U}(\mathbf{x},\mathbf{y})\,\mathbf{t}_i(\mathbf{y})\;\mathrm{d}\Gamma_i(\mathbf{y}) \qquad (2)$$

where Γ_i denotes the surface along the inclusion and $\mathbf{t}_i$ are the interaction forces (surface boundary tractions). Because the inclusion is rigid, it is subjected to rigid-body motions. The displacement **u**(**y**) at any point **y** on the inclusion can be described by the following rigid-body motions [8, 9]:

$$\mathbf{u}(\mathbf{y}) = \mathbf{d} + \boldsymbol{\omega} \times \mathbf{p}(\mathbf{y}) \tag{3}$$

where **d** is a rigid-body translation displacement vector, **ω** is a rotation vector, **p** is a position vector for point **y** measured from a reference point (for example a corner or the center of the inclusion).
Additional equations are needed to supplement equations (2). Because the considered body is in an equilibrium, therefore the corresponding equilibrium equations of forces and moments for the rigid inclusion have the following form:

$$\int_{\Gamma_i} \mathbf{t_i}(\mathbf{y})\ \mathrm{d}\Gamma_i(\mathbf{y}) = \mathbf{0} \tag{4}$$

$$\int_{\Gamma_i} \mathbf{p}(\mathbf{y}) \times \mathbf{t_i}(\mathbf{y})\ \mathrm{d}\Gamma_i(\mathbf{y}) = \mathbf{0} \tag{5}$$

In order to obtain a numerical solution, the outer boundary of the body and the surface of the inclusion are divided into quadratic boundary elements. Along the external boundary the variations of coordinates, displacements and tractions are interpolated using quadratic shape functions. Along the surface of the inclusion the variations of tractions (interaction forces) are interpolated. The collocation nodes are both the nodes on the external boundary of the body and along the surface of the inclusion.
Using equations (3), the nodal displacement vector **u** for the inclusion can be related to the rigid-body translation **d** and rotation **ω** of that inclusion by the following expression:

$$\mathbf{u} = \mathbf{I}\ \mathbf{u_i} \tag{6}$$

where **u** contains the components of displacements of the inclusion nodes, **I** depends on the position of nodes along the inclusion surface and $\mathbf{u_i}$ contains the components of the rigid-body displacements.
The equilibrium equations (4) and (5) for the inclusion can be written in a form:

$$\mathbf{E}\ \mathbf{t_i} = \mathbf{0} \tag{7}$$

where **E** contains coefficients dependent on the position of the inclusion nodes and obtained by evaluating equations (4) and (5) for that inclusion, $\mathbf{t_i}$ contains the components of nodal interaction forces (tractions) for the inclusion.
Putting all unknowns on a one side, boundary integral equations (2) supplied with equations (6) and (7) can be written in a form:

$$\begin{bmatrix} \mathbf{H_{ee}} & -\mathbf{G_{ei}} & \mathbf{0} \\ \mathbf{H_{ie}} & -\mathbf{G_{ii}} & \mathbf{I} \\ \mathbf{0} & \mathbf{E} & \mathbf{0} \end{bmatrix} \begin{bmatrix} \mathbf{u_e} \\ \mathbf{t_i} \\ \mathbf{u_i} \end{bmatrix} = \begin{bmatrix} \mathbf{G_{ee}} \\ \mathbf{G_{ie}} \\ \mathbf{0} \end{bmatrix} \left[\mathbf{t_e}\right] \tag{8}$$

where the submatrices with the index **e** and **i** refer to the external boundary and the inclusion, respectively, submatrices **H** and **G** depend on fundamental solutions and shape functions.
Finally, applying known boundary conditions, the system of equations (8) is rearranged and solved. The unknowns are displacements $\mathbf{u_e}$ and/or tractions $\mathbf{t_e}$ on the external boundary, rigid-body motions $\mathbf{u_i}$ of the inclusion and tractions $\mathbf{t_i}$ along the surface of the inclusion. The above formulation is also valid for a 2D body reinforced by a rigid-line inclusion.

3 Numerical example

A rectangular plate (2D model) and a rectangular prism (3D model) containing a straight rigid-line or a square planar rigid-surface inclusion is subjected to the uniform horizontal loading q_x or to the vertical loading q_y, as shown in Figure 1. The length and the side length of the inclusion, respectively for the 2D and 3D model, is l=3 cm. A zero-thickness model of both inclusions is assumed in the present formulation. The inclusion is located in the centre of the models along the symmetry axis/plane. The length, the height and the width (for the 3D case) is L=5 cm, H=4 cm and W=5 cm, respectively. The material of the plate (in plane strain state) or the prism has the Poisson's ratio ν=0.3 and the Young modulus $E=2\cdot10^{11}$ Pa.

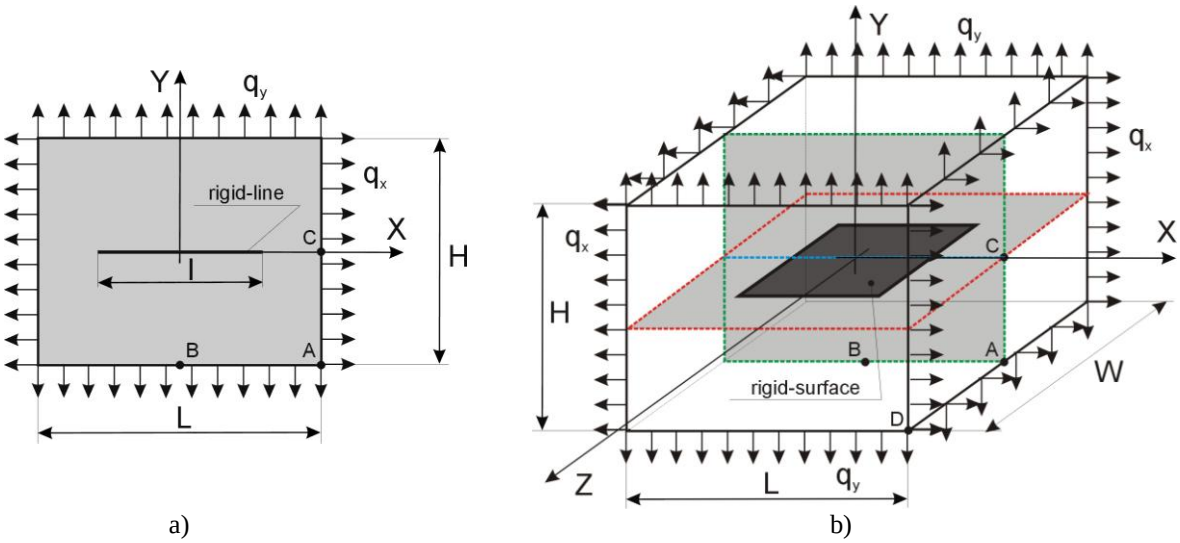

Figure 1. Rigid inclusion in a rectangular: a) plate, b) prism.

Displacements and tractions obtained by the BEM for the 2D and 3D models are computed and compared. In order to verify the formulation, displacements are additionally computed by the FEM using ANSYS system. Displacements are analyzed at selected points of the models shown in Figure 1, i.e. the points A, B, C and D. In order to show the deformed shapes, displacements are also analyzed along the outer boundary of the 2D model and along two plane sections shown in Figure 1 and marked with dashed green and red lines for the 3D model. The first plane is perpendicular to the rigid-surface inclusion and the second one is in the plane of the inclusion. These two plane sections are hereinafter called the "perpendicular plane section" and the "in-plane section". Tractions are analyzed along the rigid-line inclusion for the 2D model and along the edges of the rigid-surface inclusion for the 3D model. Displacements are normalized with respect to a scale factor u_o ($u_o=10^{-6}$ cm). Tractions are normalized with respect to the prescribed tractions q ($q_x=q_y=q=10^5$ Pa).

The outer boundary of the 2D plate is divided into 36 quadratic 3-noded boundary elements and the rigid-line inclusion into 6 elements. The outer boundary of the 3D prism is divided into 520 quadratic 8-noded BEs and the rigid-surface inclusion into 36 elements. It results in 144 and 4686 degrees of freedom (DOF) for the 2D and 3D model, respectively. The number of FEs at the side lengths of the FEM models is two times greater than the number of BEs. The corresponding models in the FEM analysis are discretized into 320 quadrilateral 8-noded and 6400 solid 20-noded finite elements, respectively, which results in 1033 and 86499 DOF, respectively.

The deformed shape of the plate (2D) and the rectangular prism in the "perpendicular plane section" (3D) is shown in Figure 2, for the two considered load cases. The deformed shape of the prism in the "in-plane section" is shown in Figure 3. An influence of the rigid inclusions on the deformation of boundaries of the models can be clearly seen.

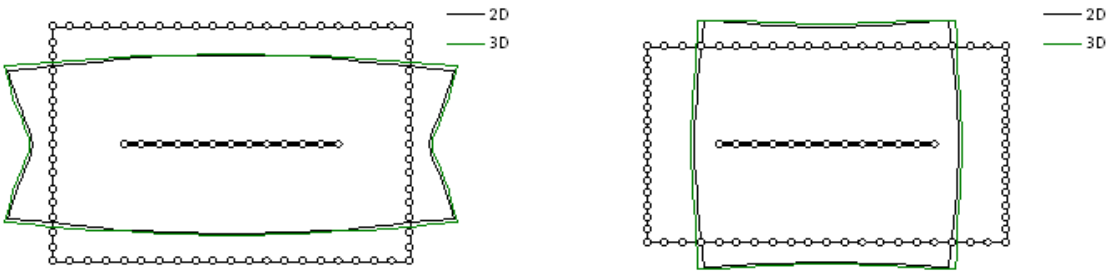

a) b)

Figure 2. Deformation of the plate (2D) and the rectangular prism in the ”perpendicular plane section” (3D): a) horizontal load q_x, b) vertical load q_y.

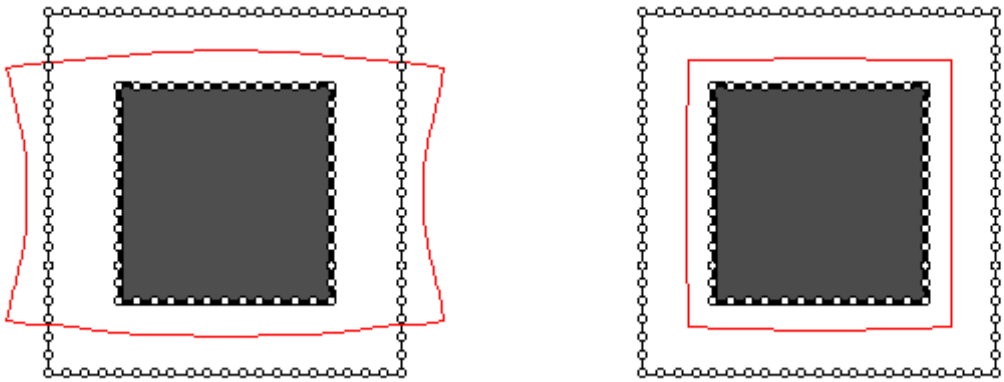

a) b)

Figure 3. Deformation of the rectangular prism in the ”in-plane section”: a) horizontal load q_x, b) vertical load q_y.

The components of the normalized displacements at the considered points of the models obtained by the BEM and FEM are presented in Table 1. A very good agreement of the BEM and the FEM results is observed for the corresponding models and loads. The results are also comparable for the 2D and 3D models however greater differences and a higher stiffness of the 2D model are noticed. This is due to the fact, that the rigid-surface inclusion in the 3D model has finite dimensions (it is a square), while in the 2D model the inclusion is infinite in the direction perpendicular to the model.

Model	Point Method	Load	A u_x/u_o	A u_y/u_o	B u_y/u_o	C u_x/u_o	D u_x/u_o	D u_y/u_o	D u_z/u_o
2D	BEM	q_x	1.1598	0.5273	0.2052	0.7596	-	-	-
	FEM	q_x	1.1594	0.5254	0.2069	0.7608	-	-	-
2D	BEM	q_y	-0.4971	-0.9688	-0.8308	-0.3255	-	-	-
	FEM	q_y	-0.4969	-0.9680	-0.8315	-0.3261	-	-	-
3D	BEM	q_x	1.2034	0.4370	0.1822	0.8116	1.3086	0.3639	-0.4261
	FEM	q_x	1.2026	0.4361	0.1841	0.8117	1.3083	0.3622	-0.4261
3D	BEM	q_y	-0.3923	-1.0072	-0.8990	-0.2795	-0.3782	-1.0548	-0.3782
	FEM	q_y	-0.3920	-1.0072	-0.9006	-0.2799	-0.3781	-1.0533	-0.3781

Table 1. Normalized displacements at selected points of 2D and 3D models.

All the tractions presented below are the forces of interaction of the rigid inclusion on the deformable matrix. The normalized tractions t_x/q_x and t_x/q_y along the rigid-line (2D) and the rigid-surface in the "perpendicular plane section" (3D) are shown in Figure 4a and 4b, respectively (tractions t_y are zero in the considered load cases). In both cases, concentrations of tractions are present at the tips (edges for the 3D) of the inclusion.

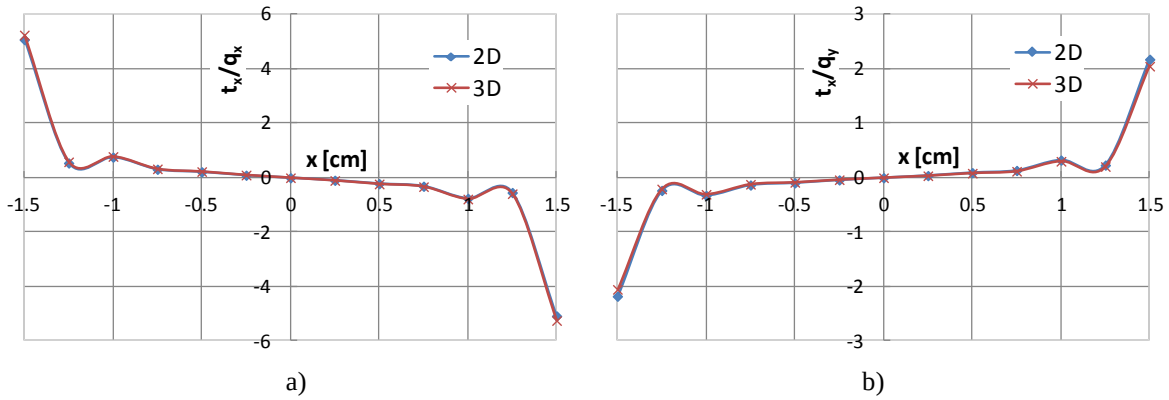

a) b)

Figure 4. Tractions along the rigid-line (2D) and the rigid-surface in "perpendicular plane section" (3D): a) horizontal load q_x – normalized tractions t_x/q_x, b) vertical load q_y – normalized tractions t_x/q_y.

The normalized tractions t_x/q_x and t_z/q_x along the edges of the rigid-surface inclusion are shown in Figure 5a and 5b, respectively. The highest concentrations of tractions are present at the corners of the inclusion.

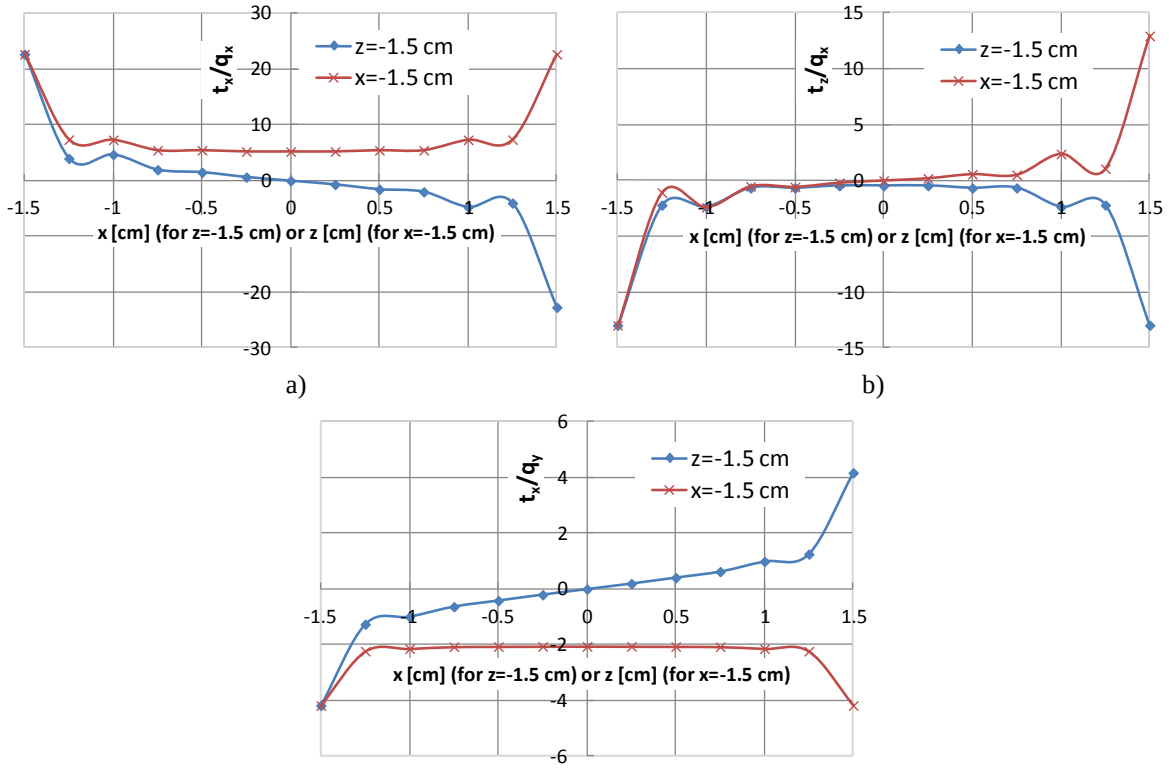

a) b)

c)

Figure 5. Tractions along the edges of the rigid-surface inclusion: a) horizontal load q_x – normalized tractions t_x/q_x, b) horizontal load q_x – normalized tractions t_z/q_x, c) vertical load q_y – normalized tractions t_x/q_y.

For the vertical load, the normalized tractions t_x/q_y along the edges of the inclusion are shown in Figure 5c (tractions t_z/q_y are symmetrical in comparison with t_x/q_y for this load). Tractions t_y are zero in both considered load cases, similar as for the 2D plate.

4 Conclusions

The formulation for the analysis of elastic bodies with rigid reinforcements is presented. The boundary element method (BEM) is used for two- and three-dimensional bodies reinforced by rigid-line and rigid-surface inclusions, respectively. The formulation is verified by comparing the results with the FEM solutions and an excellent agreement of displacements is obtained. High concentrations of tractions are present at the tips of the rigid-line and at the corners of the rigid-surface inclusions.

The method is accurate and the number of degrees of freedom is significantly reduced in comparison with domain-based methods, for instance the FEM. The method can be used in modeling of composites in which a reinforcement is much stiffer than a matrix. It can be in the form of the fiber-like (rigid-line) or the flake-like (rigid-surface) particles. The exemplary materials where such a big difference of stiffness is present are nanocomposites. Typical particles in such composites are carbon nanotubes, graphene or nanoclay layers, etc. In the numerical example a single straight or a planar perfectly rigid inclusion in an elastic medium was considered in order to show possible applications of the method. However, the method can be also applied in analysis of bodies with multiple particles of arbitrary shapes.

References

[1] Ballarini R. An integral equation approach for rigid line inhomogeneity problems. *International Journal of Fracture*, **33**, pp. 23-26 (1987).

[2] Pingle P., Sherwood J., Gorbatikh L. Properties of rigid-line inclusions as building blocks of naturally occurring composites. *Composites Science and Technology*, **68**, pp. 2267-2272 (2008).

[3] Gorbatikh L., Lomov S.V., Verpoest I. Relation between elastic properties and stress intensity factors for composites with rigid-line reinforcements. *International Journal of Fracture*, **161**, pp. 205-212 (2010).

[4] Gao X.W., Davies T.G. *Boundary element programming in mechanics*. Cambridge University Press, Cambridge (2002).

[5] Górski R. Elastic properties of composites reinforced by wavy carbon nanotubes. *Mechanics and Control*, **30**, 4, pp. 203-212 (2011).

[6] Fedeliński P. Boundary element method in analysis of elastic bodies with rigid fibers. *Engineering Modeling*, **32**, pp. 135-142 (2006) (in Polish).

[7] Fedeliński P. *Analysis of composites with multiple rigid-line reinforcements by the BEM* in ”Proceedings of Computer Methods in Mechanics CMM-2011”, Warsaw, Poland, pp. 181-182 (2011) (CD-ROM, 5 pages).

[8] Liu Y.J., Nishimura N., Otani Y., Takahashi T., Chen X.L., Munakata H. A fast boundary element method for the analysis of fiber-reinforced composites based on a rigid-inclusion model. *Journal of Applied Mechanics*, **72**, pp. 115-128 (2005).

[9] Liu Y.J., Nishimura N., Otani Y. Large-scale modeling of carbon-nanotube composites by fast multipole boundary element method. *Computational Material Science*, **34**, pp. 173-187 (2005).